

Accepted Manuscript

Comparison of different speciation techniques to measure Zn availability in hydroponic media

Encarna Companys, Josep Galceran, Jaume Puy, Maria Sedó, Ruben Vera, Enriqueta Anticó, Clàudia Fontàs



PII: S0003-2670(18)30836-5

DOI: [10.1016/j.aca.2018.06.071](https://doi.org/10.1016/j.aca.2018.06.071)

Reference: ACA 236086

To appear in: *Analytica Chimica Acta*

Received Date: 12 February 2018

Revised Date: 6 June 2018

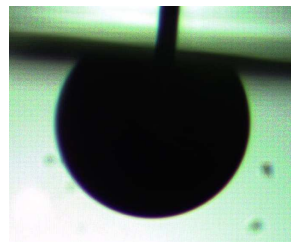
Accepted Date: 25 June 2018

Please cite this article as: E. Companys, J. Galceran, J. Puy, M. Sedó, R. Vera, E. Anticó, C. Fontàs, Comparison of different speciation techniques to measure Zn availability in hydroponic media, *Analytica Chimica Acta* (2018), doi: 10.1016/j.aca.2018.06.071.

This is a PDF file of an unedited manuscript that has been accepted for publication. As a service to our customers we are providing this early version of the manuscript. The manuscript will undergo copyediting, typesetting, and review of the resulting proof before it is published in its final form. Please note that during the production process errors may be discovered which could affect the content, and all legal disclaimers that apply to the journal pertain.

© 2018. This manuscript version is made available under the CC-BY-NC-ND 4.0 license <http://creativecommons.org/licenses/by-nc-nd/4.0/>





AGNES, free



DGT, labile



LASV, labile



PIM, free

1 **Comparison of different speciation techniques to measure Zn**
2 **availability in hydroponic media**

3 Encarna Companys^a, Josep Galceran^{a,*}, Jaume Puy^a, Maria Sedó^a, Ruben Vera^b,
4 Enriqueta Anticó^b and Clàudia Fontàs^b

5 ^a*Departament de Química. Universitat de Lleida and AGROTECNIO, Rovira Roure*
6 *191, 25198 Lleida, Spain*

7 ^b*Departament de Química, Universitat de Girona, 17071 Girona, Spain*

8 * *Corresponding author galceran@quimica.udl.cat*

9

10 **Abstract**

11 Four analytical techniques are compared: AGNES (Absence of Gradients and Nernstian
12 Equilibrium Stripping), LASV (Anodic Stripping Voltammetry with Linear stripping),
13 DGT (Diffusive Gradients in Thin films) and PIM (Polymer Inclusion Membranes).
14 These techniques have been designed to provide the free ion concentration or a labile
15 fraction, complementarily contributing to an integrated description of speciation and
16 availability. Their simultaneous application to the determination of free Zn
17 concentrations or labile fluxes in seven solutions of a hydroponic medium reveals
18 characteristics of each technique and correlations between their results. All dynamic
19 results can be interpreted in terms of a general theoretical framework on fluxes. Indeed,
20 in techniques under diffusion-limited conditions in the sample, the flux can be split into
21 the free contribution (linearly proportional to the free fraction), plus the contribution of
22 the complexes (where mobility, lability and abundance of complexation are
23 intertwined). A methodology to compute lability degrees is developed. Measurements

24 with PIM devices confirm that diffusion in the sample solution is not rate limiting, so its
25 flux is proportional to the free metal in the donor solution. A proportionality between
26 the responses of any given two techniques is observed, which suggests that, for the low
27 ligand-to-metal concentration ratios used in the present work, any of these techniques
28 would correlate similarly with uptake, toxic or nutritional measurements.

29

30 **Keywords:** Diffusive Gradients in Thin Films; Absence of Gradients and Nernstian
31 Equilibrium Stripping; Polymer Inclusion Membrane; Voltammetry; Zinc ; Speciation

32

33 **1. Introduction**

34 Hegemonic paradigms, such as the Free Ion Activity Model (FIAM) [1] and the Biotic
35 Ligand Model (BLM) [2], correlate the toxicity (or nutritional capacity) of a trace metal
36 to the free metal ion concentration (or activity) in the medium in contact with the
37 organism. However, some exceptions to this key role of the free metal ion have been
38 pointed out [3, 4]. The uptake of Zn and Cu by spinach and tomato plants, for fixed free
39 metal ion concentrations ($[Zn^{2+}]$ and $[Cu^{2+}]$), increased when more metal was also
40 bound to ligands [5], indicating that metal complexes might contribute to the uptake by
41 dissociating close to the root surface according to their lability [6]. More recent reports
42 [7-9] also indicate the contribution of complexes, either by their dissociation or by their
43 direct internalization on the roots, in some cases, while the key role of the free metal ion
44 is confirmed in most cases.

45

46 So, there is a current debate on the extent of the contribution of the different chemical
47 species towards the resulting uptake of a metal. Clearly, there is a need for knowing not
48 only the equilibrium concentrations (i.e. the distribution of the element amongst
49 different chemical species, which is called the equilibrium speciation of the element),
50 but also the rate of contribution to the uptake from the dissociation of the complexes
51 (i.e. the dynamic speciation) in the medium [10-12]. The answer to this need is the
52 development of analytical techniques able to quantify concrete fractions of an element,
53 such as the concentration of the free fraction or the so-called "labile fraction". Some of
54 these fractions have shown good correlation with the metals accumulated in plants [13-
55 15]. Central to this development is the improvement of their interpretation, i.e. the
56 assessment of which species and to which extent do they contribute to the fluxes.
57 Comprehensive reviews of the main developments of dynamic and equilibrium
58 techniques have been recently published [12, 16-19].

59

60 Free metal ion concentrations can be directly measured by a few techniques. The use of
61 an Ion Selective Electrode (ISE) [20] would be a simple way to determine the free Zn^{2+}
62 concentration, but, up to date, there is no commercial ISE for Zn. Membrane based
63 techniques have also been developed for the determination of the free metal
64 concentration. The Donnan Membrane Technique (DMT) [21] uses a cation exchange
65 membrane to measure free ion concentrations based on Donnan membrane equilibrium.
66 In the Resin Titration Technique [16] and in the Ion-Exchange Technique [22] the
67 analyte is accumulated in an ionic exchange resin. The electroanalytical technique
68 AGNES [19, 23] has proved successful in measuring the free concentration of Zn in a
69 range of systems including natural waters [24-27], dispersions of nanoparticles [28, 29]
70 or wine [30].

71 Labile fractions are accessed via the dynamic techniques. The general recorded signal of
72 these techniques is an arriving flux of metal to a sensor. Apart from the direct supply of
73 the free metal to this flux, there might be other contributions. In some cases, the
74 complexes might contribute directly (e.g. second wave in stripping techniques [31]), but
75 usually some prior dissociation of the complexes generating free metal is required [32].
76 The rate of such dissociation (in comparison with the diffusion rate) determines the so-
77 called “lability degree” (ξ) of the complex [33, 34].

78

79 One of the classical dynamic techniques is Anodic Stripping Voltammetry (ASV), with
80 many variants such as the one with the application of a linear potential scan in the
81 stripping stage (LASV). Along the deposition stage of any ASV variant, the arriving
82 metal species is reduced to M^0 forming a metal amalgam at the mercury electrode,
83 which is later on stripped from the mercury by oxidation, yielding an intensity current
84 which is the response signal [16]. The correct interpretation of such a signal remains
85 still a challenge, given complications such as the electrodic adsorption of humic matter.
86 Since time ago [35, 36] operational correlations of ASV lability and bioavailability were
87 indicated. More recent investigations have also correlated stripping signals with the
88 uptake of Zn^{2+} to a diatom [37] or to wheat roots [9].

89

90 Diffusive Gradients in Thin films (DGT) is based on the accumulation of metal in a disc
91 of gel with embedded beads of Chelex resin, while another disc of gel serves to
92 (practically) define the diffusion domain [38]. DGT has been applied to natural waters,
93 sediments and soils [8, 39] and to hydroponic media [7, 40].

94

95 The Permeation Liquid Membrane (PLM) technique relies on the selective
96 transportation of the analyte across a hydrophobic membrane via a carrier [41-43] and
97 can be tuned to determine the free species (or to some labile fraction). Polymer
98 Inclusion Membrane (PIM) is a membrane based technique where ion transfer requires
99 binding to a carrier molecule [44], similarly to PLM, but much more robust. PIM have
100 been recently shown to measure free ion concentrations [45].

101

102 The aim of the present work is to apply different techniques to determine the free (with
103 AGNES and PIM) and labile fractions (with DGT and LASV) of Zn available in
104 hydroponic medium at different concentrations of ligand (EDTA or humic acid). Zinc
105 is an essential metal for plants (and its deficiency has been reported in soils of many
106 arid regions of the world [7]), so its uptake attracts much attention. The relevant
107 medium for plants is the soil solution, which can also be approximated by hydroponic
108 media, much more controlled. Comparison of PIM, DGT and LASV results is
109 performed by converting their respective responses to fluxes [40]. Special emphasis is
110 devoted to the interpretation of the fluxes obtained with the dynamic speciation
111 techniques.

112 **2. Materials and Methods**

113 **2.1 Reagents**

114 For the preparation of the nutrient solution the following reagents were used:
115 $\text{KNO}_3 \cdot 4\text{H}_2\text{O}$, $\text{Ca}(\text{NO}_3)_2$, KH_2PO_4 , $\text{MgSO}_4 \cdot 7\text{H}_2\text{O}$, NH_4NO_3 , H_3BO_3 , $\text{MnCl}_2 \cdot 4\text{H}_2\text{O}$,
116 $\text{CuSO}_4 \cdot 5\text{H}_2\text{O}$, $\text{Na}_2\text{MoO}_4 \cdot 2\text{H}_2\text{O}$, $\text{ZnSO}_4 \cdot 7\text{H}_2\text{O}$; they were all purchased from Panreac
117 (Barcelona, Spain). As an iron source, the commercial product Kelamix Fe was used

118 (Sicosa, Girona, Spain). According to the producing company, 6% of the mass
119 corresponds to Fe, which is chelated by ethylenediamine-N,N'-bis(2-
120 hydroxyphenylacetic acid) (EDDHA); but the complete formulation is undisclosed. The
121 ESI-MS spectra of the product are shown in Fig SI-1. The buffer employed was 2-(N-
122 morpholino) ethanesulfonic acid (MES) obtained from Fluka (Bern, Switzerland).
123 Organic ligands such as humic acid sodium salt (technical grade, HA) and EDTA were
124 provided by Sigma-Aldrich (St Louis, Missouri, USA). Elemental composition of HA,
125 used as received, is presented in Table SI-1.

126

127 For PIM preparation, the polymer polyvinyl chloride (PVC) and the carrier di-2-
128 ethylhexyl phosphoric acid (D2EHPA) were from Fluka (Bern, Switzerland) and
129 Sigma-Aldrich (St Louis, Missouri, USA), respectively. Tetrahydrofuran (THF) solvent
130 was from Panreac (Barcelona, Spain).

131

132 A standard solution 1000 mg L⁻¹ Zn (Merck, Darmstadt, Germany) and solid KNO₃
133 (Fluka, St Louis, USA) TraceSelect grade were used to prepare the calibration standards
134 for AGNES and LASV.

135

136 HNO₃ 69% (Fisher Chemical, Loughborough, UK) was used for DGT elutions prior to
137 ICP-MS analysis. A standard solution 1000 mg L⁻¹ Zn (High Purity Standards,
138 Charleston, USA) was used to prepare the calibration standards for ICP-MS.

139

140 All reagents and solvents used in this study were of analytical grade except the ones
141 whose different quality has been specified.

142

143 Ultrapure water with 18 M Ω cm resistivity (Synergy UV purification system Millipore)
144 was used in all preparations.

145

146 2.2 Preparation of hydroponic media

147 The nutrient solution was based on Hoagland growth medium [46]. The concentrations
148 were modified by dilution to reach a final composition as follows: 2.5 mmol L⁻¹
149 KNO₃·4H₂O, 2.5 mmol L⁻¹ Ca(NO₃)₂, 0.25 mmol L⁻¹ KH₂PO₄, 1 mmol L⁻¹
150 MgSO₄·7H₂O, 0.5 mmol L⁻¹ NH₄NO₃, 23 μ mol L⁻¹ H₃BO₃, 4.2 μ mol L⁻¹ MnCl₂·4H₂O,
151 0.1 μ M CuSO₄·5H₂O, 0.25 μ mol L⁻¹ Na₂MoO₄·2H₂O, 0.38 μ mol L⁻¹ ZnSO₄·7H₂O, and
152 12 μ mol L⁻¹ Fe (from Kelamix). This solution composition is referred to as half-
153 strength Hoagland medium. The pH was adjusted to 6.0 \pm 0.1 by using 2.5 mmol L⁻¹
154 MES buffer. It has been reported that MES does not complex Zn significantly [47].

155

156 Different media have been considered in this work, with Zn added according to a
157 previous work [45] and EDTA or HA concentrations to provide similar [Zn²⁺]:

158 i. The control medium, with the composition detailed above.

159 ii. The control medium with an added Zn concentration: either 35.0 μ mol L⁻¹ (Zn₁) or
160 69.6 μ mol L⁻¹ (Zn₂), added as ZnSO₄·7H₂O.

161 iii. The medium with added Zn ($35.0 \mu\text{mol L}^{-1}$ and $69.6 \mu\text{mol L}^{-1}$), and also with the
162 presence of $20 \mu\text{mol L}^{-1}$ EDTA (Zn+EDTA_1 and Zn+EDTA_2, respectively).

163 iv. The medium with added Zn ($35.0 \mu\text{mol L}^{-1}$ and $69.6 \mu\text{mol L}^{-1}$), and also with the
164 presence of 60 mg L^{-1} humic acid (Zn+HA_1 and Zn+HA_2, respectively).

165

166 2.3 Experimental setups and instrumentation

167 PIMs containing 70% PVC and 30%D2EHPA were prepared using a procedure similar
168 to that reported by Sugiura [48]. Briefly, 400 mg of PVC were weighted and dissolved
169 in 12 mL of THF. After two hours stirring, one mL of the carrier solution, 0.5 mol L^{-1}
170 D2EHPA in THF, was added to the mixture and stirred for 1 more hour. Finally, the
171 resulting mixture was poured into a 9.0 cm diameter flat bottom glass petri dish, which
172 was set horizontally and covered loosely. The organic solvent was allowed to evaporate
173 over 24 h at room temperature, and the resulting film was carefully peeled off from the
174 bottom of the petri dish. Circular pieces of 2 cm diameter were cut from the centre of
175 the membrane and were, then, incorporated in a dedicated device, used as passive
176 sampler [45]. The membrane device was partially immersed in 250 mL of the
177 hydroponic solution under study, which was contained in a glass beaker placed on a
178 magnetic stirrer, whereas 5 mL of 0.01 mol L^{-1} HNO_3 was used as acceptor phase. After
179 a given contact time, the device was removed from the solution and the nitric acid
180 solution was analyzed for total Zn content using a sequential inductively coupled
181 plasma atomic emission spectrometer (ICP-AES) (Liberty RL, Varian, Mulgrave, Vic.,
182 Australia). PIM determinations were run at room temperature ($23 \pm 1^\circ\text{C}$).

183

184 AGNES and LASV voltammetric measurements were carried out with Eco Chemie
185 Autolab PGSTAT101 and μ Autolab Type III potentiostats attached to Metrohm 663VA
186 Stands being controlled from a computer by means of the NOVA 1.11 software. The
187 working electrode was a Metrohm multimode mercury drop electrode. The smallest
188 drop in our stand was chosen, which according to the catalogue corresponds to a radius
189 around $r_0 = 1.41 \times 10^{-4}$ m. The auxiliary electrode was a glassy carbon electrode and the
190 reference electrode was Ag/AgCl/3 mol L⁻¹ KCl, encased in a jacket containing 0.1 mol
191 L⁻¹ KNO₃.

192

193 A glass combined electrode (Crison) was attached to an Orion Research 720A+ or to an
194 Orion Dual Star ion analyzer (Thermo) and introduced in the cell to control the pH. A
195 glass jacketed cell provided by Metrohm was used in all measurements. The vessel was
196 thermostated at 25.0 °C.

197

198 DGT holders (piston type, 2 cm diameter window), polyacrylamide gel discs (diffusive
199 disc, 0.8 mm thick, and Chelex resin disc, 0.4 mm thick) from DGT Research Ltd and
200 cellulose nitrate membrane filters (0.45 μ m Whatman) were used. DGT devices were
201 prepared as described elsewhere[49]. The sensors have been left to equilibrate in a
202 solution at the same pH and ionic strength as the sample (0.011 mol L⁻¹ KNO₃ and 2.5
203 mmol L⁻¹ MES) for at least 18 hours (see Supporting Information of ref. [49]). After
204 that, the sensors have been deployed, for 24 and 48 h, inside a plastic bucket containing
205 2 L of medium kept at 240 rpm stirring rate and at 25.0°C in a thermostated bath.
206 Deployment solutions and metal accumulations (once eluted with HNO₃) in DGT

207 experiments were analysed, in triplicate, with an ICP-MS 7700x (Agilent
208 Technologies, Inc, Tokyo, Japan).

209

210 2.4 Procedures

211 2.4.1 Determination of free Zn concentrations with AGNES

212 AGNES consists in applying two stages [23, 29]: i) A first stage where we apply a
213 deposition potential for a long enough time to reach Absence of Gradients in the
214 concentration profiles and Nernstian Equilibrium at the electrode surface (these specific
215 conditions are the main difference with other stripping techniques, like LASV); and ii) a
216 second stage where we apply a reoxidation program and we measure the total charge or
217 the diffusion-limited current after a certain time. In this work, we use the variant
218 AGNES-I where the reoxidation program is a (constant) potential pulse under diffusion-
219 limited conditions and we measure the current.

220

221 At the end of the first stage a preconcentration factor Y has been achieved

$$222 \quad Y = \frac{[M^0]}{[M^{2+}]} = \exp\left[-\frac{2F}{RT}(E_1 - E^0)\right] \quad (1)$$

223 where F is the Faraday constant, R the gas constant, T the temperature, E_1 is the applied
224 deposition potential and E^0 the standard formal potential of the redox couple. Y is the
225 gain in metal concentration across the surface due to its preconcentration in the
226 amalgam following the application of E_1 and, in practise, is usually computed from the
227 peak potential of an ancillary Differential Pulse Polarogram (DPP) with just metal and
228 the background electrolyte.

229

230 The measurement of the faradaic current in the second stage allows the quantification of
231 the free metal ion concentration

$$232 \quad I_f = \eta Y [M^{2+}] \quad (2)$$

233 where I_f is the faradaic current (obtained from the subtraction of the blank to the total
234 current) and η is the normalised proportionality factor.

235

236 Prior to AGNES measurements, a calibration to obtain η is needed at the same ionic
237 strength as the sample. The calibrations were performed at 0.011 M KNO₃ given the
238 predictions of Visual MINTEQ [50] with the composition of the hydroponic medium
239 described in Section 2.2.

240

241 The quantification of the free metal concentration in each hydroponic medium has been
242 performed applying AGNES with two different Y -values as an extra checking. The Y
243 ranged from 2 to 200 depending on the free concentration. For the control medium (the
244 lowest free Zn concentration) Y of 100 and 200 were required. Only for this medium, to
245 avoid large deposition times, AGNES with 2 Pulses in the deposition stage [51] was
246 applied with $t_{1,a} = 70$ s and $t_{1,b} = 210$ s (when preconcentrating to $Y=100$) or $t_{1,a}=140$ s
247 and $t_{1,b}=420$ s (when aiming at $Y=200$). In all the cases, the waiting time at the desired
248 gain (Y) without stirring was 50 s and the preconcentration factor applied in the
249 stripping stage was 10^{-8} .

250

251 2.4.2 Determination of labile fluxes with LASV using linear stripping scan

252 Essentially, LASV technique provides an accumulation resulting from the flux of
253 analyte under diffusion-limited conditions acting throughout the deposition time.
254 Indeed, the very negative potential during the deposition stage creates a flux, due to the
255 reduction -at the electrode surface- of Zn^{2+} (resulting directly from the free Zn flux or
256 from the diffusion and dissociation of labile complexes). Steady state can be assumed
257 during this deposition stage due to the vigorous stirring in the electrochemical cell and
258 the short life of the transient regime. The linear stripping scan quantifies the amount of
259 Zn^0 accumulated in the amalgam (which corresponds to the steady-state accumulation
260 during the deposition stage plus a small amount of Zn^0 accumulated at the beginning of
261 the linear stripping scan, when the stripping potential is still close to the deposition one,
262 before Zn^0 re-oxidation starts), without further complications (as in the Differential
263 Pulse mode, where repeated oxidation/reduction cycles are much more difficult to
264 interpret). The interfering impact of adsorption (e.g. humic acid complexes on the
265 electrode surface) on the final stripped charge in this variant of LASV is expected to be
266 mild, because diffusion-limited conditions in the deposition stage hinder electrodic
267 adsorption [52] and any possible adsorption along the stripping step might distort a
268 transient intensity current, but not the final charge (that, due to Faraday law, has to be
269 proportional to the total accumulated concentration of Zn^0).

270

271 In the first stage of the LASV experiment, a deposition potential of -1.3V is applied
272 during 60 s, followed -in the second stage- by a linear scan from -1.3V to 0 V at a scan
273 rate of $0.0198 \text{ V s}^{-1}(v)$ which produces a peak in the I vs E representation. The area of
274 the peak is measured and allows the determination of the flux (J) as

$$275 \quad J = \frac{Q}{2FAt} = \frac{Area_{LASVpeak}}{v2FAt} \quad (3)$$

276 where Q is the charge (corresponding to the moles of reoxidated metal) which can be
277 obtained from the peak area $Area_{LASVpeak}$ and the scan rate (v). A is the surface area of
278 the mercury electrode (0.25 mm^2) and t is the deposition time.

279

280 2.4.3 Determination of labile fluxes with DGT

281 Under the assumption of steady-state regime along the deployment time (which will be
282 checked for the hydroponic systems), the flux (J) can be computed from the number of
283 (measured) accumulated moles of analyte in the resin disc, n_{Zn} , with the expression [53]:

$$284 \quad J = \frac{n_{Zn}}{At} \quad (4)$$

285 where A is the area of the opening (3.14 cm^2) and t the deployment time.

286

287 In many works, the accumulation of the analyte into the binding phase is associated
288 with a labile fraction or the so-called DGT-concentration c_{DGT} [53] assuming a steady-
289 state regime under diffusion-limited conditions:

$$290 \quad J = \frac{D_M c_{DGT}}{\delta^g} \quad (5)$$

291 where D_M is the diffusion coefficient of the metal analyte and δ^g is the thickness of the
292 diffusion domain (usually the aggregate thickness of disc gel, filter and diffusive
293 boundary layer).

294

295

296 **2.4.4 Determination of free concentration with PIM**

297 The PIM technique is based on carrier-mediated transport of the metal across the
298 polymeric membrane. The carrier, D2EHPA in this case, forms a neutral complex with
299 the Zn^{2+} ion at the membrane/donor interface. Then, the complex diffuses across the
300 membrane, and when reaching the membrane/acceptor interface, the metal is released
301 into the acceptor phase due to the protonation of the carrier in the aqueous phase with
302 existing HNO_3 . This chemical pumping allows the accumulation of the analyte in the
303 acceptor solution. Recent work [45] has proposed that there is a co-limitation by
304 transport both across the membrane and in the acceptor solution (rather than a limitation
305 by diffusion in the source solution), leading to an accumulation proportional to the free
306 ion concentration in the source solution, analogously to some cases of the PLM
307 technique.

308

309 **3. Results and discussion**310 **3.1 Free concentration and fluxes provided by each technique**

311 The free Zn concentration in the different hydroponic media considered in this work has
312 been determined with AGNES (see Fig 1 or Table SI-2), using the parameters detailed
313 in section 2.4.1. The $[Zn^{2+}]$ found in the control medium, $0.111 \mu mol L^{-1}$, is negligible
314 in front of the free concentrations in media with spiked Zn. As expected, the free Zn
315 concentration increases when increasing the total metal concentration of the medium
316 (compare full and empty blue square markers in Fig 1), while the free Zn concentration
317 decreases with the addition of a ligand like EDTA (red triangles) or humic acid (green

318 circles). For the conditions and concentrations considered in this work, 60 mg L⁻¹ humic
319 acid (equivalent to a concentration of sites of 342 μmol L⁻¹, according to the generic
320 parameters of the NICA-Donnan model [54]) binds less Zn than 20 μmol L⁻¹ EDTA,
321 given the found lower free Zn concentrations in the EDTA-enriched solutions.

322

323 For the sake of simplicity, when quantifying the contribution of the different complexes,
324 one can consider that the Hoagland medium acts as an equivalent ligand (labelled
325 “Hoag”) to form an effective 1:1 complex labelled “MHoag”. We neglect any variation
326 of the effective free ligand due to its complexation with the metal (the so-called ligand
327 excess conditions), so that

$$328 \quad c_{\text{MHoag}} \approx K' c_{\text{M}} \quad (6)$$

329 where K' is the excess (conditional) stability constant (or stability coefficient). The
330 mass balance (when other complexes are still not added) can be written as

$$331 \quad c_{\text{T,M}} = c_{\text{M}} + c_{\text{MHoag}} = (1 + K') c_{\text{M}} \quad (7)$$

332 K' has been evaluated as 0.21 ± 0.06 from the regression of the data (free and total) of
333 AGNES experiments with the control and with just added Zn (i.e. Zn_1 and Zn_2),
334 while also forcing the regression to pass through the origin. Using only one K' for the
335 Hoagland mixture is valid, for example, when the free concentrations of all participating
336 ligands (including EDDHA not bound to Fe) are constant despite Zn complexation. The
337 linearity observed in the plot $c_{\text{T,M}}$ vs c_{M} lends support to the use of just one K' as a first
338 approximation to describe the binding properties of the Hoagland medium.

339

340 Fluxes recorded with LASV followed a similar pattern to the concentrations measured
341 with AGNES (see Table SI-2 in Supporting Information, and Fig 2): lower fluxes for
342 lower total concentrations or solutions with an added ligand. The flux computed with
343 eqn. (3) from the LASV peak area measured in the control medium was $10.3 \text{ nmol m}^{-2}\text{s}^{-1}$.
344 The flux of Zn₂ is approximately twice that of Zn₁, consistent with the
345 approximation of labile complexation with the Hoagland medium. The decrease (with
346 respect to fluxes of Zn₁ and Zn₂) due to EDTA addition is similar for both total Zn
347 concentrations, as expected for a formed strong inert complex. The impact of EDTA in
348 reducing the analytical signal is, again, more important than that of humic acid.

349

350 For DGT, the accumulations were measured after 24 and 48 h. The almost direct
351 proportionality between accumulation and deployment time seen in Fig. 3 indicates that
352 the system is under steady-state regime. Under these conditions, equation (4) can be
353 applied to compute the flux. DGT fluxes follow a similar trend to the free
354 concentrations measured with AGNES: the presence of EDTA or HA reduce the
355 accumulation (for a given time) as seen in Fig. 3. The reduction of the flux due to the
356 addition of a ligand can be understood as due to a partial complexation of the Zn ions,
357 leading to a reduced availability (compared with that resulting if the total concentration
358 of Zn was free). This decrease in availability can be due to a much lower diffusion
359 coefficient of the complex (the expected case for a macromolecular entity like humic
360 acid diffusing in a gel), due to a lower lability degree (the expected case for EDTA), as
361 described below in section 3.2 or due to a combination of both effects. From the point
362 of view of DGT, the fluxes with EDTA and HA have essentially the same value (within
363 experimental error) which is compatible with the diffusion coefficient of ZnHA being
364 smaller than that of ZnEDTA.

365

366 As with DGT technique, the direct proportionality between accumulation and
367 deployment time seen in Fig. SI-2 for PIM experiments indicates that the system is
368 under steady-state regime and can be computed with using equation (4). PIM fluxes due
369 to ligand additions can be seen in Fig. 4 and can be interpreted along the lines of the
370 previous paragraph. In agreement with the measurements of the other techniques, J_{PIM}
371 decreases when EDTA is added, as expected for the formation of a complex, and
372 remains below J_{PIM} corresponding to the system with HA. Moreover, the declines in the
373 computed fluxes due to the addition of EDTA or humic acid are similar to those seen
374 with AGNES, LASV and DGT.

375

376 3.2. Relationship between the information provided by different techniques

377 The interpretative framework developed for DGT (see, for instance [53]) can be
378 extended to other techniques yielding fluxes. A key idea is to split the total flux of metal
379 into the contribution from the free metal (J_{free} , represented as dotted lines in Figs. 5-6)
380 plus the contribution from the complexes. These complexes can be classified as those
381 complexes existing in the Hoagland medium and those complexes due to a ligand
382 addition (EDTA and HA), with the general label ML:

$$383 \quad J = J_{\text{total}} = J_{\text{free}} + J_{\text{Hoag}} + J_{\text{ML}} = \frac{D_{\text{M}}}{\delta} c_{\text{M}} + \frac{D_{\text{Hoag}}}{\delta} c_{\text{MHoag}} \xi_{\text{Hoag}} + \frac{D_{\text{ML}}}{\delta} c_{\text{ML}} \xi_{\text{ML}} \quad (8)$$

384 where D_i is the diffusion coefficient of the species (free metal, M; complex with the
385 medium MHoag; complex with added ligand, ML), c_i is the concentration of each
386 species, ξ_i is the lability degree of each species (see Introduction), and δ is the

387 thickness of the diffusion layer of the technique. In DGT, δ corresponds to the
388 summation of gel, filter and Diffusive Boundary Layer thicknesses, while in LASV δ
389 will depend on the stirring rate with no fixed term. If one considers δ an operational
390 parameter to reproduce fluxes in well defined hydrodynamic regimes (such as laminar
391 flow), it will depend on (some powers of) the diffusion coefficients of the participating
392 species [55, 56]. However, turbulence (or natural convection due to local
393 inhomogeneities in temperature or density of solution) renders the consideration of
394 laminar flow also approximate, supporting the rough first approximation of considering
395 δ as fixed. This is the satisfactory standard approach to deal with the DBL in DGT [57].
396 For PIM, eqn. (8) would apply if the limiting step was diffusion in the solution. On the
397 other hand, if the limiting step is not diffusion in the solution, then the flux does not
398 contain any information on the lability or amount of complexes in the sample, but just
399 on the free metal ion[45].

400

401 Given that the ligands of the Hoagland medium are not macromolecular, one can
402 assume $D_{\text{Hoag}}=D_{\text{M}}$. As the expected (inorganic) complexes of Zn with the medium are
403 weak, one can assume that they are fully labile, so $\xi_{\text{Hoag}}=1$. Combining eqns. (8) and
404 (7):

$$405 \quad J = \frac{D_{\text{M}}}{\delta} (1 + K') c_{\text{M}} + \frac{D_{\text{ML}}}{\delta} c_{\text{ML}} \xi_{\text{ML}} \quad (9)$$

406

407 From the particular case of experiments Zn_1 and Zn_2 (i.e. when $c_{\text{ML}}=0$), one can
408 compute D_{M} / δ which could be called the flux factor

$$409 \quad \frac{D_M}{\delta} = \frac{J}{c_M(1+K')} = \frac{J}{c_{T,M}} \quad (10)$$

410

411 For DGT, the experimentally retrieved flux factor ($0.52 \times 10^{-6} \text{ m s}^{-1}$) is close to the
 412 theoretical one ($0.55 \times 10^{-6} \text{ m s}^{-1}$) computed from $D_{\text{Zn}} = 6.08 \times 10^{-10} \text{ m}^2 \text{ s}^{-1}$ for Zn diffusion
 413 in the gel (from DGT research website) and $\delta = 1.1 \text{ mm}$. For LASV, $(D_M/\delta)_{\text{exp}} = 3.4 \times 10^{-5}$
 414 m s^{-1} while $(D_M/\delta)_{\text{theor}} = 3.6 \times 10^{-5} \text{ m s}^{-1}$ (taking $\delta_{\text{LASV}} = 2 \times 10^{-5} \text{ m}$ [23, 58, 59] and
 415 $D_{\text{Zn}} = 7.3 \times 10^{-10} \text{ m}^2 \text{ s}^{-1}$ for Zn diffusion in water).

416

417 According to equation (9), a representation of the flux in terms of the free metal
 418 concentration, for solutions where the second term was negligible, would yield a
 419 straight line passing through the origin. Such a “medium line” can be drawn from the
 420 experimental flux factor of each technique and the obtained K' (see brown continuous
 421 lines in Figs. 5-6). These lines should go through markers corresponding to Zn_1 and
 422 Zn_2 (square blue markers), which is approximately the case in Figs. 5-6.

423

424 The ordinate difference between any of the rest of experimental markers and this brown
 425 continuous line can be called “offset” and physically corresponds to the contribution to
 426 the flux of the complex (other than the complexes with the medium, MHoag) expressed
 427 by the last term in eqn. (9):

$$428 \quad J_{\text{ML}} = \xi_{\text{ML}} \frac{D_{\text{ML}} c_{\text{ML}}}{\delta} \quad ((11))$$

429

430 For cases with an added ligand, the lability degree can be computed from the
431 corresponding offset of the marker with respect to the medium line (brown continuous
432 line), just by solving for ξ_{ML} in eqn (11) and taking c_{ML} as:

$$433 \quad c_{ML} = c_{T,M} - c_M (1 + K') \quad (12)$$

434

435 In the technique DGT, see Fig 5, EDTA offsets can be converted into lability degrees by
436 assuming $D_{ML}=D_M$. For the low Zn concentration, one finds $\xi_{EDTA}=0.31$, while for the
437 higher concentration $\xi_{EDTA}=0.60$. The difference has to be mostly ascribed to
438 experimental errors and inaccuracies in the input parameters (total concentrations, free
439 concentration, K' , DGT fluxes, etc.) required for the calculations. Indeed, as most of the
440 analytical signal (i.e. the flux) comes from the free Zn concentration, the small
441 difference between the total and this free contribution (i.e. the offset) accumulates
442 (relatively) large uncertainties. The key conclusion is a rather low ξ_{EDTA} , consistent with
443 the inert nature of ZnEDTA, but it could also be consistent with an insufficient effective
444 affinity of Zn for the iminodiacetic resin (of the Chelex resin used in our DGT) in front
445 of the strong ligand (EDTA), see [60, 61].

446

447 To extract lability degrees for HA complexes from the offsets, we take
448 $D_M=D_{Zn}=6.08 \times 10^{-10} \text{ m}^2\text{s}^{-1}$ and $D_{ML}=4.77 \times 10^{-10} \text{ m}^2\text{s}^{-1}$ (average value of the range
449 reported recently [62]) which lead to a ratio $D_{ML}/D_M=0.78$.

450

451 For the probed HA solutions with DGT, Fig 5, assuming $D_{ML}=0.78 \times D_M$, the offsets
452 translate to $\xi_{HA}=0.10$ for Zn+HA_1 and $\xi_{HA}=0.99$ for Zn+HA_2, respectively. The

453 increase of the lability degree of humic acid when the Zn concentration increases can be
454 understood due to the increasing occupation by Zn ions of humic sites with decreasing
455 affinity. Assuming Eigen's complexation mechanism [63], a decrease in the affinity of a
456 site can be ascribed to an increase of the dissociation rate constant, increasing in this
457 way the lability. For the higher concentration of the present work, ξ_{HA} is higher than for
458 EDTA, in broad agreement with some quite labile behaviour reported for Zn complexes
459 with humic acids [64]. Notice that the knowledge of the diffusion coefficient value is
460 necessary to compute the lability degree. In this regard, an equation previously used in
461 the literature, eqn (7) in [5] and eqn. (6) in [9] would not be valid for a complex with a
462 diffusion coefficient different from that of the metal (as it is the case with HA). The
463 equation can be corrected as follows:

$$464 \quad \xi_{\text{ML}} = \left(\frac{J}{J_{\text{free}}} - 1 \right) \frac{c_{\text{M}}}{D_{\text{ML}} c_{\text{ML}}} \quad (13)$$

465 where J_{free} is the flux obtained in a system which has only metal and whose free
466 concentration is just the same as in the solution where there is also the complex. This
467 equation is not applied in this work because this special solution with just metal has not
468 been prepared.

469

470 For the technique LASV, triangle markers in Fig 6 reflect a positive offset for
471 Zn+EDTA_1, while for the higher concentration, the offset is negative. As both are of
472 the same order of magnitude, and considering that a negative offset renders meaningless
473 any computation with Eqn. ((11), we can conclude that the lability degree of ZnEDTA
474 is close to zero for this technique. The offsets for HA are too disperse to be subject to a
475 qualitative mathematical analysis. We speculate that perhaps a low reproducibility of

476 stirring between days (which impacts on the thickness of the diffusion layer) might be
477 responsible for an accuracy insufficient for the low ligand to metal ratio of these
478 experiments.

479

480 One can highlight that the lability degree of a complex is not an intrinsic property of the
481 complex, but it is also sensor and technique dependent. Actually, the lability depends
482 not only on the ability of the complex to dissociate (dissociation rate constant,
483 composition of the media), but also on the spatial and time scale where this dissociation
484 takes place (e.g. the characteristics of the sensor) [65].

485

486 A well-known effect is that lability increases when the thickness of the diffusion layer
487 increases [33, 65]. Thus, one expects that lability degrees measured by DGT are higher
488 than those measured by LASV in the same chemical system, because the main
489 difference between both techniques is the thickness of the diffusion layer (of the order
490 of 1.1 mm for DGT and just 20 μm for LASV [58]). Additionally, the penetration of
491 complexes in the resin disc, where free metal is absent and dissociation proceeds,
492 renders them more labile in DGT [66, 67]. Although this is the trend of ξ values
493 obtained above for EDTA, unfortunately, they do not allow a clear confirmation of this
494 expectation. In this respect, DGT computations of the lability degree are more trustable,
495 because of the smaller variation between experiments and a better defined value of δ in
496 the technique.

497

498 In the PIM technique, eqn. (8) does not apply, because the flux is not determined by
499 diffusion in the solution [45]. So, with PIM -despite measuring a flux - no information
500 on the lability of the complexes in the solution can be gained. Fig 7 confirms -within
501 the experimental error- the proportionality between PIM fluxes and the measurements
502 of free Zn concentrations provided by AGNES. This is expected from PIM fluxes being
503 proportional to the free Zn concentration [45].

504

505 If we compare now directly the results between techniques, we observe that DGT and
506 LASV are very well correlated (see Fig 8). The LASV fluxes also correlate well with
507 PIM fluxes (see Fig SI-3). These correlations can be attributed to the low ligand to
508 metal ratio used in these experiments.

509

510 **4. Conclusions**

511 Equation (9) supports the representation (seen in Figs 5, and 6) of the fluxes in front of
512 the free ion concentration (provided by AGNES or PIM). The last term in Equation (9)
513 is visualized as the distance (or offset) between a marker and the line corresponding to
514 the contribution of the fixed ligands of the medium. From this last term, lability degree
515 can be computed, though more work is needed to obtain more reliable estimates. Those
516 lability degrees derived here from DGT measurement are the most robust, probably
517 because of the better controlled thickness of the diffusion layer.

518

519 The results from this work (see Fig 7) confirm that, in these conditions, PIM can be
520 used to measure free metal ion concentrations. So, plots like Figs 5 and 6 could also be

521 drawn taking as abscissae the values of the PIM fluxes (or its conversion into free
522 concentrations via a calibration) instead of AGNES free concentrations.

523

524 In principle, the different techniques provide access to different fractions of the
525 analyzed system and their information can be considered as complementary [32].
526 However, for some conditions, the differences might be not large enough to be
527 quantified. This leads to a kind of equivalence of the techniques (for such systems)
528 which results in more robust and confirmed conclusions when there is general
529 agreement between them. Due to this equivalence (under the present conditions this
530 might be related to a relative large proportion of free Zn in comparison with the
531 complexed forms), other criteria for selecting a technique can be adopted. For instance,
532 the application of LASV with the mercury electrode has the advantage of the reduced
533 time of the experiment when compared with DGT and PIM. LASV does not requires the
534 analysis with a complementary technique (ICP-MS or ICP-OES). On the other hand,
535 DGT and PIM can be applied *in situ*, which avoids contaminations in sampling and
536 storage (though there is also a transport of the accumulated analyte towards the
537 laboratory for an instrumental analysis).

538

539

540 The found correlations between the assayed techniques also suggests that in some
541 systems, like the one shown here, a correlation between the results of one technique
542 with a particular plant uptake or toxicity might not be proof of the free metal or a given
543 labile fraction being their relevant determinant.

544

545 **Acknowledgements**

546 This work was financially supported by the Spanish Ministry of Education and Science
547 (projects CTM2013-48967 and CTM2016-78798). Alexandra Altier's help with DGT
548 experiments is acknowledged.

549 **Supplementary data**

550 Electronic supplementary information related to this article can be found at
551 <http://dx.doi.org/XXXXX>.

552

553

Literature cited

- 554 1. M. A. Anderson, F. M. M. Morel, R. R. L. Guillard, Growth limitation of a coastal
555 diatom by low zinc ion activity, *Nature*, 276 (1978) 70-71.
- 556 2. P. R. Paquin, J. W. Gorsuch, S. Apte, G. E. Batley, K. C. Bowles, P. G. C.
557 Campbell, C. G. Delos, D. M. Di Toro, R. L. Dwyer, F. Galvez, R. W. Gensemer,
558 G. G. Goss, C. Hogstrand, C. R. Janssen, J. C. McGeer, R. B. Naddy, R. C. Playle,
559 R. C. Santore, U. Schneider, W. A. Stubblefield, C. M. Wood, K. B. Wu, The
560 biotic ligand model: a historical overview, *Comp. Biochem. Physiol. C*, 133
561 (2002) 3-35.
- 562 3. A. Larbi, F. Morales, A. Abadia, Y. Gogorcena, J. J. Lucena, J. Abadia, Effects of
563 Cd and Pb in sugar beet plants grown in nutrient solution: induced Fe deficiency
564 and growth inhibition, *Functional Plant Biology*, 29 (2002) 1453-1464.
- 565 4. C. M. Zhao, P. G. C. Campbell, K. J. Wilkinson, When are metal complexes
566 bioavailable?, *Environ. Chem.*, 13 (2016) 425-433.
- 567 5. F. Degryse, E. Smolders, D. R. Parker, Metal complexes increase uptake of Zn
568 and Cu by plants: implications for uptake and deficiency studies in chelator-
569 buffered solutions, *Plant Soil*, 289 (2006) 171-185.
- 570 6. F. Degryse, E. Smolders, R. Merckx, Labile Cd complexes increase Cd
571 availability to plants, *Environ. Sci. Technol.*, 40 (2006) 830-836.
- 572 7. A. Gramlich, S. Tandy, E. Frossard, J. Eikenberg, R. Schulin, Diffusive limitation
573 of zinc fluxes into wheat roots, PLM and DGT devices in the presence of organic
574 ligands, *Environ. Chem.*, 11 (2014) 41-50.
- 575 8. J. Luo, H. Zhang, F. J. Zhao, W. Davison, Distinguishing Diffusional and Plant
576 Control of Cd and Ni Uptake by Hyperaccumulator and Nonhyperaccumulator
577 Plants, *Environmental Science & Technology*, 44 (2010) 6636-6641.
- 578 9. P. Wang, D. M. Zhou, X. S. Luo, L. Z. Li, Effects of Zn-complexes on zinc uptake
579 by wheat (*Triticum aestivum*) roots: a comprehensive consideration of physical,
580 chemical and biological processes on biouptake, *Plant Soil*, 316 (2009) 177-192.
- 581 10. R. Albajes, C. Cantero-Martinez, T. Capell, P. Christou, A. Farre, J. Galceran, F.
582 López-Gatius, S. Marin, O. Martin-Belloso, M. J. Motilva, C. Nogareda, J. Peman,
583 J. Puy, J. Recasens, I. Romagosa, M. P. Romero, V. Sanchis, R. Savin, G. A.
584 Slafer, R. Soliva-Fortuny, I. Viñas, J. Voltas, Building bridges: an integrated
585 strategy for sustainable food production throughout the value chain, *Molecular*
586 *Breeding*, 32 (2013) 743-770.
- 587 11. P. Bradac, R. Behra, L. Sigg, Accumulation of Cadmium in Periphyton under
588 Various Freshwater Speciation Conditions, *Environmental Science & Technology*,
589 43 (2009) 7291-7296.

- 590 12. A. M. Mota, J. P. Pinheiro, M. L. S. Goncalves, Electrochemical Methods for
591 Speciation of Trace Elements in Marine Waters. Dynamic Aspects, *J. Phys. Chem.*
592 *A*, 116 (2012) 6433-6442.
- 593 13. F. Degryse, E. Smolders, H. Zhang, W. Davison, Predicting availability of mineral
594 elements to plants with the DGT technique: a review of experimental data and
595 interpretation by modelling, *Environ. Chem.*, 6 (2009) 198-218.
- 596 14. J. H. Ren, P. N. Williams, J. Luo, H. R. Ma, X. R. Wang, Sediment metal
597 bioavailability in Lake Taihu, China: evaluation of sequential extraction, DGT,
598 and PBET techniques, *Environ. Sci. Pollut. R.*, 22 (2015) 12919-12928.
- 599 15. A. Gramlich, S. Tandy, C. Gauggel, M. Lopez, D. Perla, V. Gonzalez, R. Schulin,
600 Soil cadmium uptake by cocoa in Honduras, *Sci. Total Envir.*, 612 (2018) 370-
601 378.
- 602 16. M. Pesavento, G. Alberti, R. Biesuz, Analytical methods for determination of free
603 metal ion concentration, labile species fraction and metal complexation capacity of
604 environmental waters: A review, *Anal. Chim. Acta*, 631 (2009) 129-141.
- 605 17. J. Feldmann, P. Salaun, E. Lombi, Critical review perspective: elemental
606 speciation analysis methods in environmental chemistry - moving towards
607 methodological integration, *Environ. Chem.*, 6 (2009) 275-289.
- 608 18. R. F. Domingos, A. Gelabert, S. Carreira, A. Cordeiro, Y. Sivry, M. F. Benedetti,
609 Metals in the Aquatic Environment-Interactions and Implications for the
610 Speciation and Bioavailability: A Critical Overview, *Aquat. Geochem.*, 21 (2015)
611 231-257.
- 612 19. E. Companys, J. Galceran, J. P. Pinheiro, J. Puy, P. Salaun, A review on
613 electrochemical methods for trace metal speciation in environmental media,
614 *Current Opinion in Electrochemistry*, 3 (2017) 144-162.
- 615 20. E. Bakker, E. Pretsch, *Modern Potentiometry*, *Angew. Chem. , Int. Ed.*, 46 (2007)
616 5660-5668.
- 617 21. E. J. M. Temminghoff, A. C. C. Plette, R. van Eck, W. H. van Riemsdijk,
618 Determination of the chemical speciation of trace metals in aqueous systems by
619 the Wageningen Donnan Membrane Technique, *Anal. Chim. Acta*, 417 (2000)
620 149-157.
- 621 22. C. Fortin, F. Caron, Complexing capacity of low-level radioactive waste leachates
622 for Co-60 and Cd-109 using an ion-exchange technique, *Anal. Chim. Acta*, 410
623 (2000) 107-117.
- 624 23. J. Galceran, E. Companys, J. Puy, J. Cecilia, J. L. Garcés, AGNES: a new
625 electroanalytical technique for measuring free metal ion concentration, *J.*
626 *Electroanal. Chem.*, 566 (2004) 95-109.
- 627 24. D. Chito, L. Weng, J. Galceran, E. Companys, J. Puy, W. H. van Riemsdijk, H. P.
628 van Leeuwen, Determination of free Zn^{2+} concentration in synthetic and natural
629 samples with AGNES (Absence of Gradients and Nernstian Equilibrium

- 630 Stripping) and DMT (Donnan Membrane Technique), *Sci. Total Envir.*, 421-422
631 (2012) 238-244.
- 632 25. C. Parat, L. Authier, A. Castetbon, D. Aguilar, E. Companys, J. Puy, J. Galceran,
633 M. Potin-Gautier, Free Zn²⁺ determination in natural freshwaters of the Pyrenees:
634 towards on-site measurements with AGNES, *Environ. Chem.*, 12 (2015) 329-337.
- 635 26. H. B. C. Pearson, J. Galceran, E. Companys, C. Braungardt, P. Worsfold, J. Puy,
636 S. Comber, Absence of Gradients and Nernstian Equilibrium Stripping (AGNES)
637 for the determination of [Zn²⁺] in estuarine waters, *Anal. Chim. Acta*, 912 (2016)
638 32-40.
- 639 27. J. Galceran, C. Huidobro, E. Companys, G. Alberti, AGNES: a technique for
640 determining the concentration of free metal ions. The case of Zn(II) in coastal
641 Mediterranean seawater., *Talanta*, 71 (2007) 1795-1803.
- 642 28. C. David, J. Galceran, C. Rey-Castro, J. Puy, E. Companys, J. Salvador, J. Monné,
643 R. Wallace, A. Vakourov, Dissolution kinetics and solubility of ZnO nanoparticles
644 followed by AGNES., *J. Phys. Chem. C*, 116 (2012) 11758-11767.
- 645 29. J. Galceran, M. Lao, C. David, E. Companys, C. Rey-Castro, J. Salvador, J. Puy,
646 The impact of electrodic adsorption on Zn, Cd or Pb speciation measurements
647 with AGNES, *J. Electroanal. Chem.*, 722-723 (2014) 110-118.
- 648 30. E. Companys, M. Naval-Sanchez, N. Martinez-Micaelo, J. Puy, J. Galceran,
649 Measurement of free zinc concentration in wine with AGNES, *J. Agric. Food*
650 *Chem.*, 56 (2008) 8296-8302.
- 651 31. G. Alberti, R. Biesuz, C. Huidobro, E. Companys, J. Puy, J. Galceran, A
652 comparison between the determination of free Pb(II) by two techniques: Absence
653 of Gradients and Nernstian Equilibrium Stripping and Resin Titration, *Anal.*
654 *Chim. Acta*, 599 (2007) 41-50.
- 655 32. L. Sigg, F. Black, J. Buffle, J. Cao, R. Cleven, W. Davison, J. Galceran, P.
656 Gunkel, E. Kalis, D. Kistler, M. Martin, S. Noel, Y. Nur, N. Odzak, J. Puy, W. H.
657 van Riemsdijk, E. Temminghoff, M. L. Tercier-Waeber, S. Toepperwien, R. M.
658 Town, E. Unsworth, K. W. Warnken, L. P. Weng, H. B. Xue, H. Zhang,
659 Comparison of analytical techniques for dynamic trace metal speciation in natural
660 freshwaters, *Environ. Sci. Technol.*, 40 (2006) 1934-1941.
- 661 33. J. Galceran, J. Puy, J. Salvador, J. Cecilia, H. P. van Leeuwen, Voltammetric
662 lability of metal complexes at spherical microelectrodes with various radii, *J.*
663 *Electroanal. Chem.*, 505 (2001) 85-94.
- 664 34. J. Puy, J. Galceran, Theoretical aspects of dynamic metal speciation with
665 electrochemical techniques, *Current Opinion in Electrochemistry*, 1 (2017) 80-87.
- 666 35. G. E. Batley, S. C. Apte, J. L. Stauber, Speciation and bioavailability of trace
667 metals in water: Progress since 1982, *Aust. J. Chem.*, 57 (2004) 903-919.

- 668 36. O. M. Lage, H. M. V. M. Soares, M. T. S. D. Vasconcelos, A. M. Parente, R.
669 Salema, Toxicity effects of copper(II) on the marine dinoflagellate *Amphidinium*
670 *carterae*: Influence of metal speciation, *Eur. J. Phycol.*, 31 (1996) 341-348.
- 671 37. J. M. Kim, O. Baars, F. M. M. Morel, The effect of acidification on the
672 bioavailability and electrochemical lability of zinc in seawater, *Philosophical*
673 *Transactions of the Royal Society A-Mathematical Physical and Engineering*
674 *Sciences*, 374 (2016).
- 675 38. W. Davison, H. Zhang, In-situ speciation measurements of trace components in
676 natural- waters using thin-film gels, *Nature*, 367 (1994) 546-548.
- 677 39. A. A. Menegario, L. N. M. Yabuki, K. S. Luko, P. N. Williams, D. M. Blackburn,
678 Use of diffusive gradient in thin films for in situ measurements: A review on the
679 progress in chemical fractionation, speciation and bioavailability of metals in
680 waters, *Anal. Chim. Acta*, 983 (2017) 54-66.
- 681 40. M. Jakl, J. J. Dyrtrtova, D. Miholova, D. Kolihoiva, J. Szakova, P. Tlustos, Passive
682 diffusion assessment of cadmium and lead accumulation by plants in hydroponic
683 systems, *Chemical Speciation and Bioavailability*, 21 (2009) 111-120.
- 684 41. N. Parthasarathy, J. Buffle, Capabilities of supported liquid membranes for metal
685 speciation in natural-waters - application to copper speciation, *Anal. Chim. Acta*,
686 284 (1994) 649-659.
- 687 42. L. Tomaszewski, J. Buffle, J. Galceran, Theoretical and analytical characterisation
688 of a flow-through permeation liquid membrane with well-controlled flux for metal
689 speciation measurements, *Anal. Chem.*, 75 (2003) 893-900.
- 690 43. A. Gramlich, S. Tandy, V. I. Slaveykova, A. Duffner, R. Schulin, The use of
691 permeation liquid membranes for free zinc measurements in aqueous solution,
692 *Environ. Chem.*, 9 (2012) 429-437.
- 693 44. R. Guell, E. Antico, S. D. Kolev, J. Benavente, V. Salvado, C. Fontas,
694 Development and characterization of polymer inclusion membranes for the
695 separation and speciation of inorganic As species, *J. Membrane Sci.*, 383 (2011)
696 88-95.
- 697 45. R. Vera, C. Fontàs, J. Galceran, O. Serra, E. Anticó, Polymer inclusion membrane
698 to access Zn speciation: Comparison with root uptake, *Sci. Total Envir.*, 622-623
699 (2018) 316-324.
- 700 46. D. R. Hoagland, D. I. Arnon, University of California, College of Agriculture,
701 Agricultural Experiment Station., Berkeley, CA (USA), 1950.
- 702 47. H. M. V. M. Soares, S. C. Pinho, M. G. R. T. M. Barros, Influence of N-
703 Substituted Aminosulfonic Acids with a Morpholinic Ring pH Buffers on the
704 Redox Processes of Copper or Zinc Ions: A Contribution to Speciation Studies,
705 *Electroanal.*, 11 (1999) 1312-1317.

- 706 48. M. Sugiura, Transport of Lanthanide Ions through Cellulose Triacetate
707 Membranes Containing Hinokitiol and Flavonol as Carriers, *Sep. Sci. Technol.*, 25
708 (1990) 1189-1199.
- 709 49. J. Puy, J. Galceran, S. Cruz-Gonzalez, C. A. David, R. Uribe, C. Lin, H. Zhang,
710 W. Davison, Metal accumulation in DGT: Impact of ionic strength and kinetics of
711 dissociation of complexes in the resin domain, *Anal. Chem.*, 86 (2014) 7740-7748.
- 712 50. Gustafsson, J. P. Visual MINTEQ version 3.0. <[www.lwr.kth.se/English/](http://www.lwr.kth.se/English/Oursoftware/vminteq/index.htm)
713 [Oursoftware/vminteq/index.htm](http://www.lwr.kth.se/English/Oursoftware/vminteq/index.htm)> 2010
- 714 51. E. Companys, J. Cecilia, G. Codina, J. Puy, J. Galceran, Determination of the
715 concentration of free Zn²⁺ with AGNES using different strategies to reduce the
716 deposition time., *J. Electroanal. Chem.*, 576 (2005) 21-32.
- 717 52. J. Galceran, D. Rene, J. Salvador, J. Puy, M. Esteban, F. Mas, Reverse Pulse
718 Polarography of labile metal + macromolecule systems with induced reactant
719 adsorption - Theoretical analysis and determination of complexation and
720 adsorption parameters, *J. Electroanal. Chem.*, 375 (1994) 307-318.
- 721 53. J. Galceran, J. Puy, Interpretation of diffusion gradients in thin films (DGT)
722 measurements: a systematic approach, *Environ. Chem.*, 12 (2015) 112-122.
- 723 54. C. J. Milne, D. G. Kinniburgh, W. H. van Riemsdijk, E. Tipping, Generic NICA-
724 Donnan model parameters for metal-ion binding by humic substances, *Environ.*
725 *Sci. Technol.*, 37 (2003) 958-971.
- 726 55. H. P. van Leeuwen, J. Galceran, in H.P.van Leeuwen, W.Koester (Eds.),
727 Physicochemical kinetics and transport at chemical-biological surfaces, vol. 9,
728 John Wiley, Chichester, UK, 2004, Ch.3.
- 729 56. J. P. Pinheiro, H. P. van Leeuwen, Metal speciation dynamics and bioavailability.
730 2. Radial diffusion effects in the microorganism range, *Environ. Sci. Technol.*, 35
731 (2001) 894-900.
- 732 57. K. W. Warnken, W. Davison, H. Zhang, J. Galceran, J. Puy, In situ measurements
733 of metal complex exchange kinetics in freshwater, *Environ. Sci. Technol.*, 41
734 (2007) 3179-3185.
- 735 58. M. G. Bugarin, A. M. Mota, J. P. Pinheiro, M. L. S. Gonçalves, Influence of metal
736 concentration at the electrode surface in Differential-Pulse Anodic-Stripping
737 Voltammetry in the presence of humic matter, *Anal. Chim. Acta*, 294 (1994) 271-
738 281.
- 739 59. R. M. Town, H. P. van Leeuwen, Fundamental features of metal ion determination
740 by stripping chronopotentiometry, *J. Electroanal. Chem.*, 509 (2001) 58-65.
- 741 60. S. Mongin, R. Uribe, C. Rey-Castro, J. Cecilia, J. Galceran, J. Puy, Limits of the
742 Linear Accumulation Regime of DGT Sensors, *Environ. Sci. Technol.*, 47 (2013)
743 10438-10445.

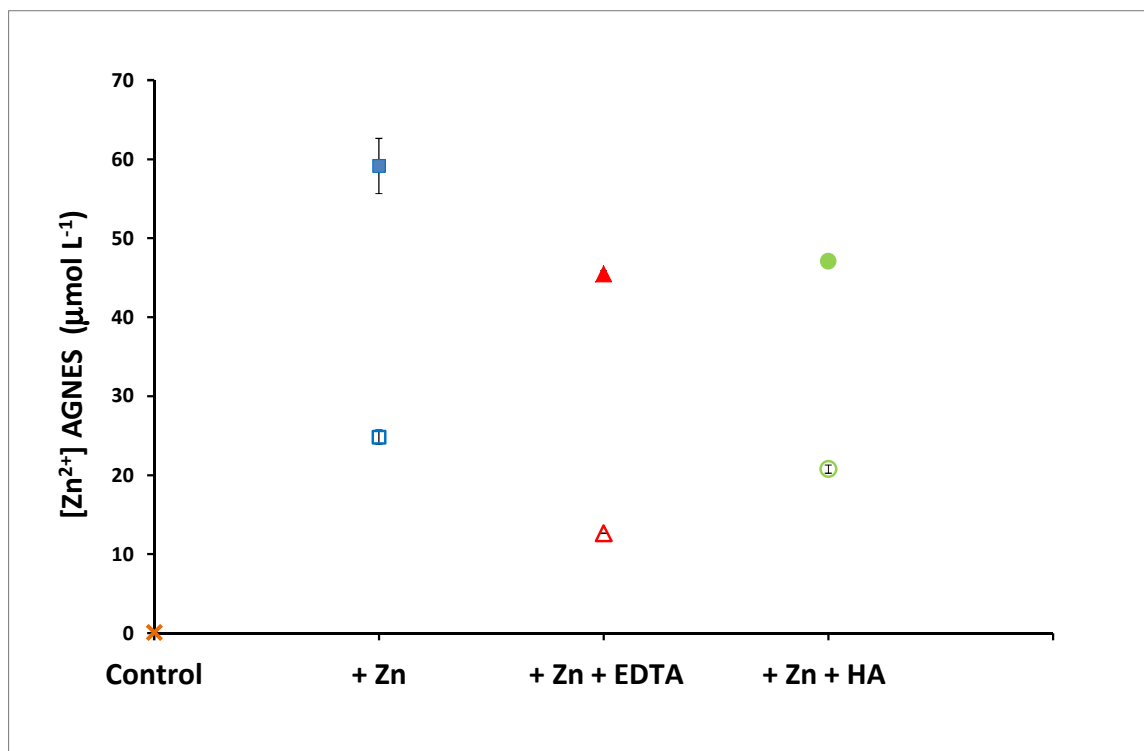
- 744 61. J. Puy, J. Galceran, C. Rey-Castro, in W. Davison (Ed.), Diffusive Gradients in
745 Thin-Films for Environmental Measurements, Cambridge University Press,
746 Cambridge, 2016, Ch.5.
- 747 62. J. Balch, C. Gueguen, Effects of molecular weight on the diffusion coefficient of
748 aquatic dissolved organic matter and humic substances, *Chemosphere*, 119 (2015)
749 498-503.
- 750 63. M. Eigen, R. Wilkins, The Kinetics and Mechanism of Formation of Metal
751 Complexes, 49 ed., American Chemical Society, Washington, 1965.
- 752 64. E. Companys, J. Puy, J. Galceran, Humic acid complexation to Zn and Cd
753 determined with the new electroanalytical technique AGNES, *Environ. Chem.*, 4
754 (2007) 347-354.
- 755 65. H. P. van Leeuwen, R. M. Town, J. Buffle, R. Cleven, W. Davison, J. Puy, W. H.
756 van Riemsdijk, L. Sigg, Dynamic speciation analysis and Bioavailability of metals
757 in Aquatic Systems, *Environ. Sci. Technol.*, 39 (2005) 8545-8585.
- 758 66. S. Mongin, R. Uribe, J. Puy, J. Cecilia, J. Galceran, H. Zhang, W. Davison, Key
759 Role of the Resin Layer Thickness in the Lability of Complexes Measured by
760 DGT, *Environ. Sci. Technol.*, 45 (2011) 4869-4875.
- 761 67. R. Uribe, S. Mongin, J. Puy, J. Cecilia, J. Galceran, H. Zhang, W. Davison,
762 Contribution of Partially Labile Complexes to the DGT Metal Flux, *Environ. Sci.*
763 *Technol.*, 45 (2011) 5317-5322.

764

765

766

Figures



767

768 Figure 1. Free [Zn²⁺] measured with AGNES in the different hydroponic media. Empty
769 markers correspond to an added $c_{T,Zn} = 3.50 \times 10^{-5}$ mol L⁻¹ and full markers to 6.96×10^{-5} mol
770 L⁻¹. Orange cross: control medium (see Section 2.2); blue squares: control media with an
771 added extra Zn concentration; red triangles: control media with added Zn and EDTA (20
772 $\mu\text{mol L}^{-1}$); green circles: control media with added Zn and humic acid (60 mg L⁻¹). Error
773 bars represent the standard deviation (if larger than the markers) corresponding to
774 replicates of two independent samples.

775

776

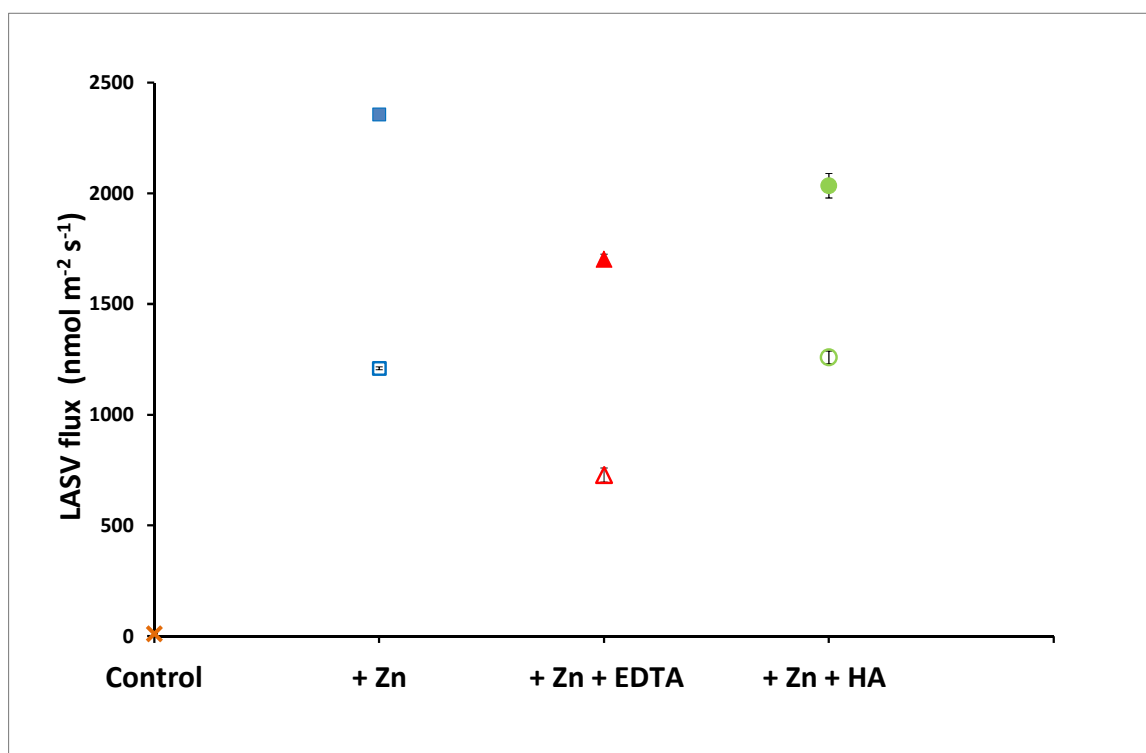
777

778

779

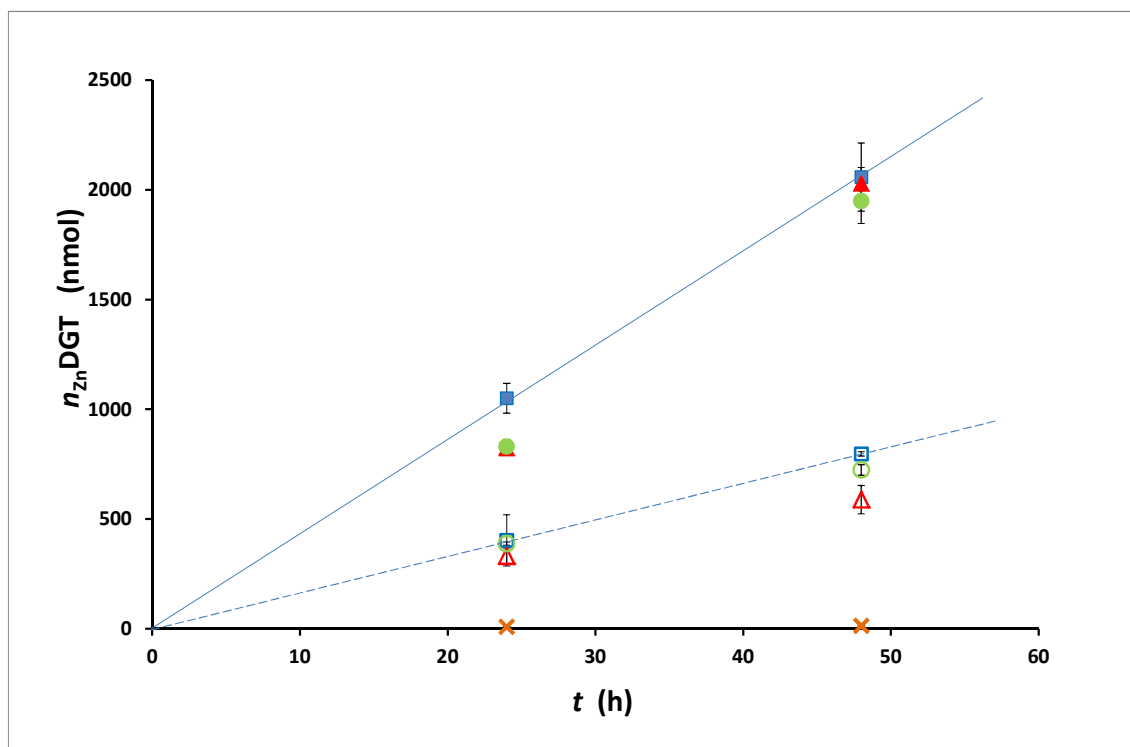
780

781

782
783

784 Figure 2: Zn flux measured with LASV (with linear stripping) in the different media.
785 Markers as in Fig 1. Error bars represent the standard deviations ($n=3$), whenever larger
786 than the marker, corresponding to different determinations in the same sample.

787

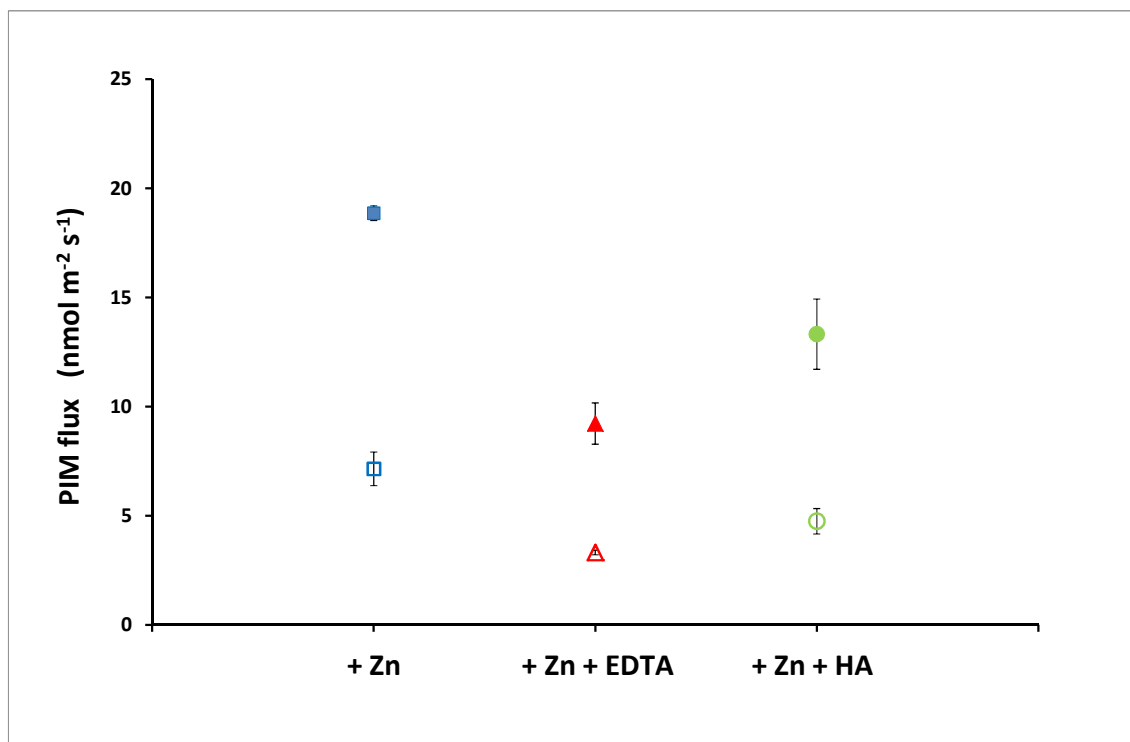


788

789

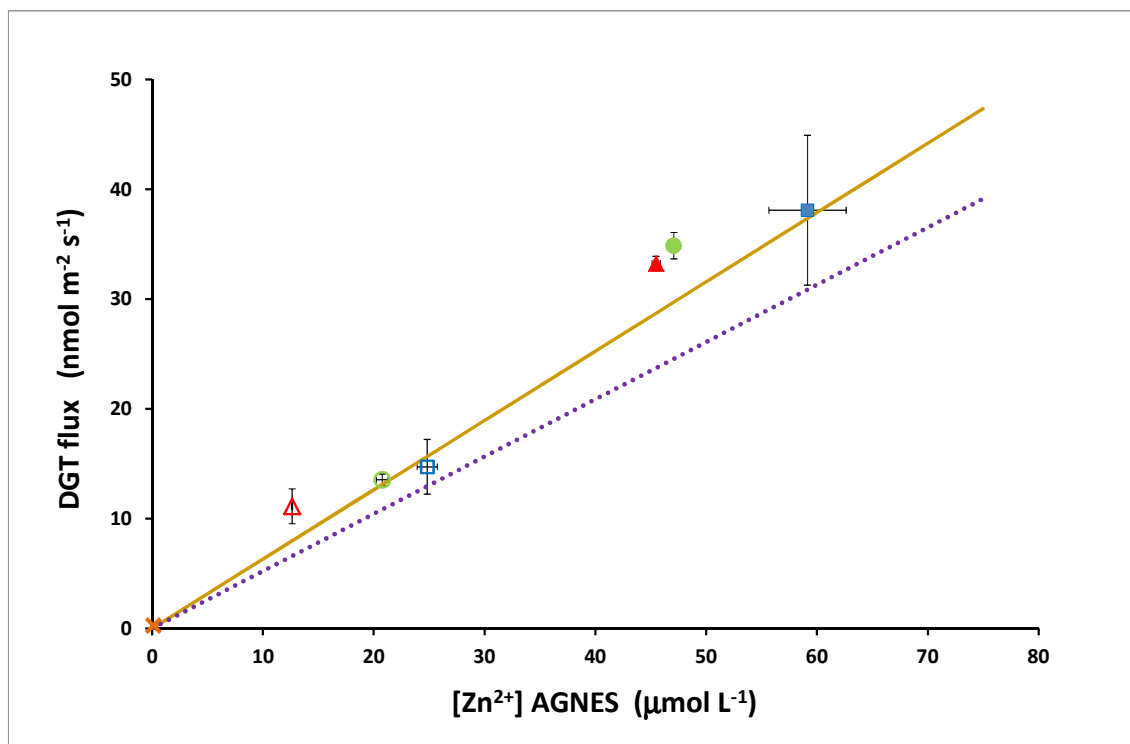
790 Figure 3. Zn accumulated in DGT devices after 24 and 48 h. Markers as in Fig 1. Lines are
791 an aid to the eye to show the linear regime for the case with just added metal. Error bars
792 represent the standard deviations ($n=3$), whenever larger than the marker, corresponding
793 to different determinations in the same sample.

794



795

796 Figure 4. Zn flux measured with PIM-based devices in the different media. Markers as in
797 Fig 1. Error bars represent the standard deviations ($n=2$ or 3) corresponding to replicates
798 of three independent samples.



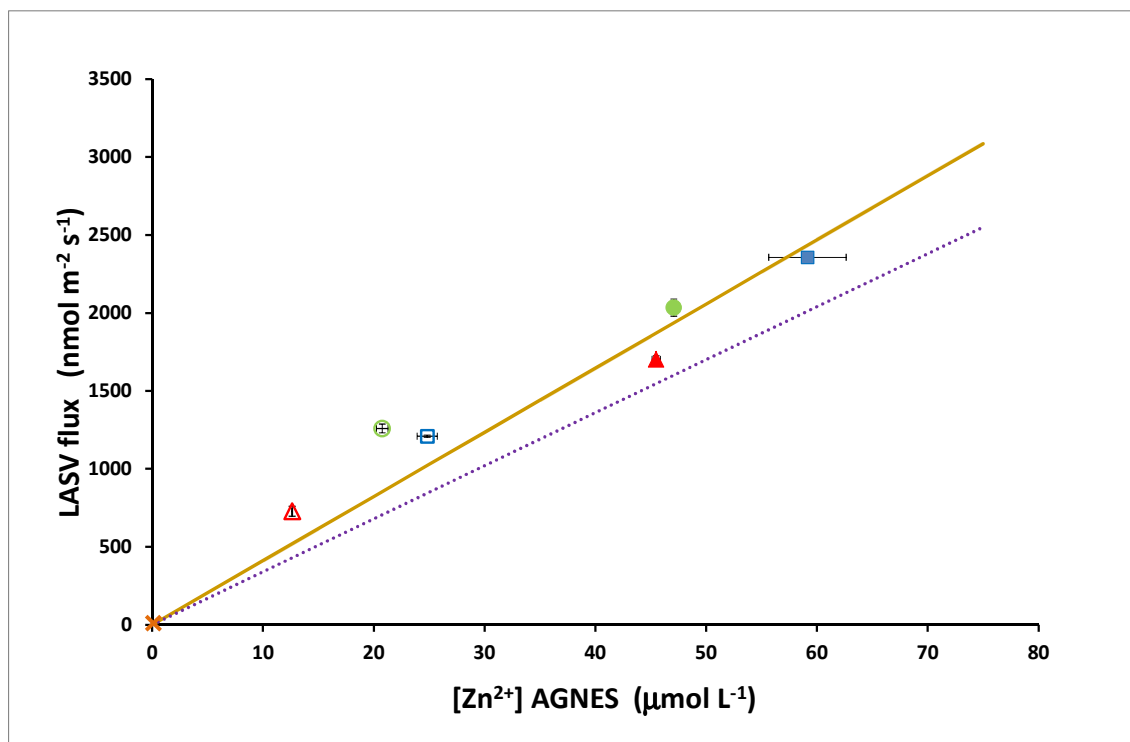
799

800 Figure 5. Zn flux with DGT versus free Zn concentration with AGNES. Markers as in Fig 1.

801 Error bars as in previous figures. The brown continuous line quantifies the contribution to
 802 the flux of free metal plus the complexes in the Hoagland medium, i.e.

803 $J_{\text{medium}} = \frac{D_M}{\delta} (1 + K') c_M$. The purple dotted line quantifies the free metal contribution to

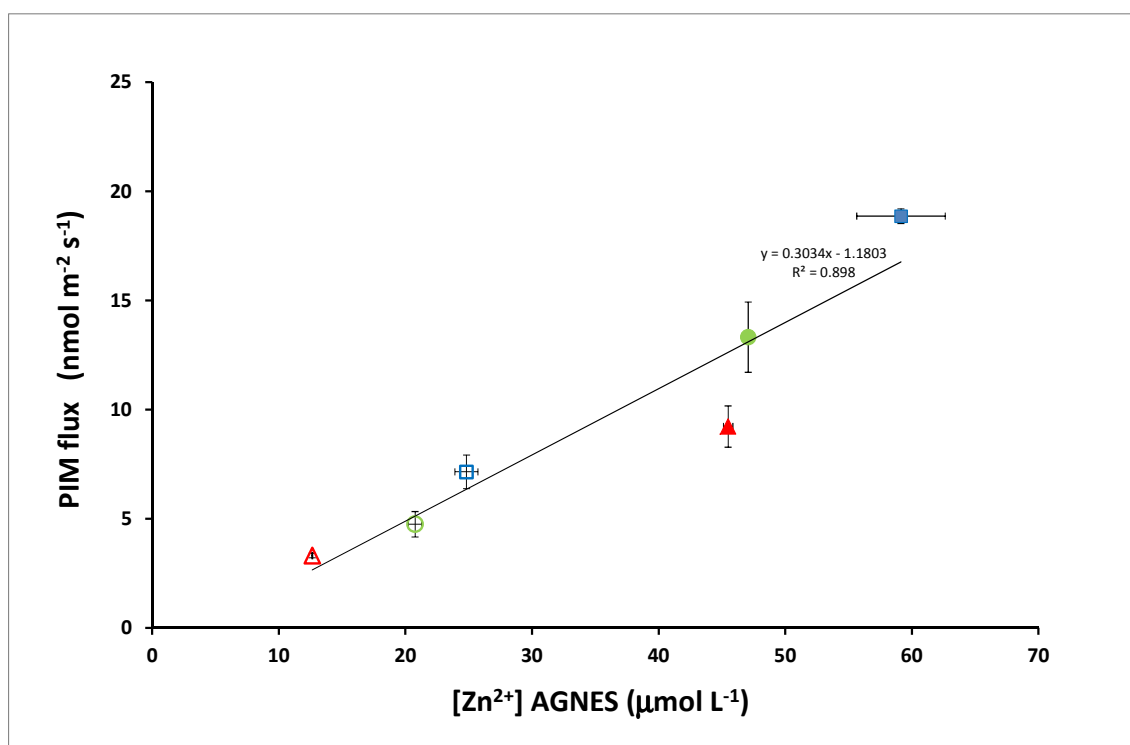
804 the flux, i.e. $J_{\text{free}} = \frac{D_M}{\delta} c_M$ with D_M / δ obtained from equation (10).



805

806 Figure 6. Zn flux obtained with LASV versus free Zn concentration obtained with AGNES.

807 Markers as in Fig 1. Error bars as in previous figures. Lines as in previous figure.

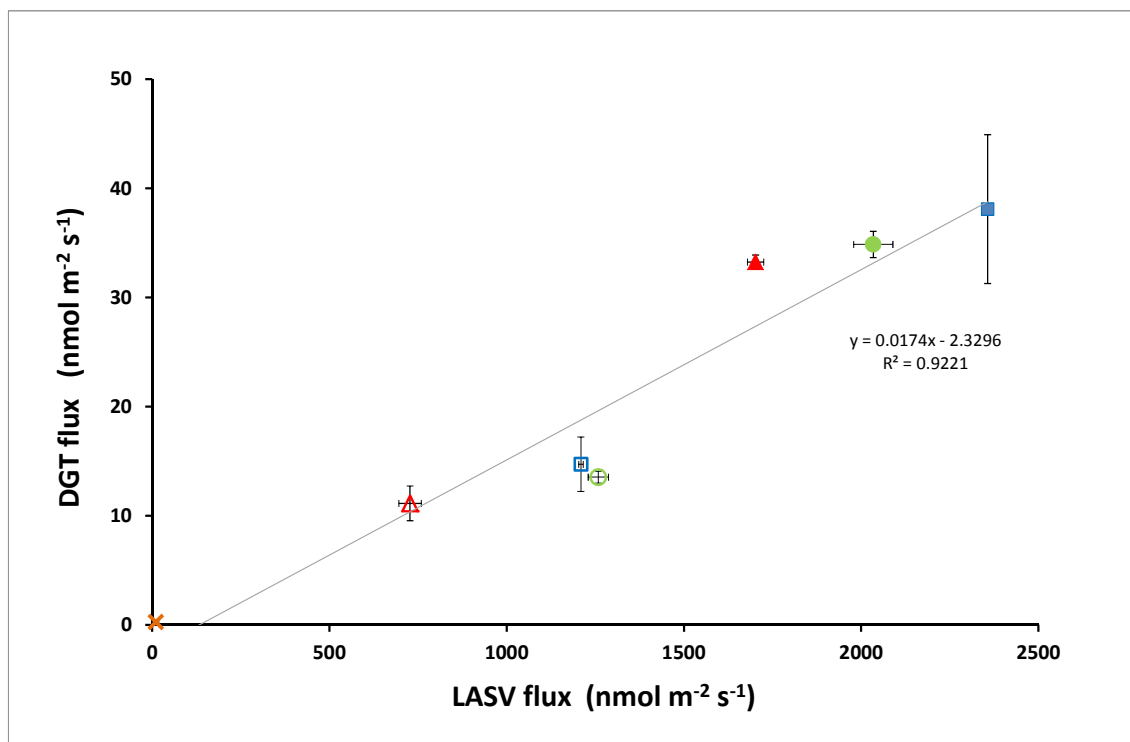


808

809 Figure 7. Zn flux measured with PIM versus free Zn concentration with AGNES. Markers as
810 in Fig 1. Error bars as in previous figures . The added straight line is the global regression
811 of the plotted data .

812

813



814

815 Figure 8. Zn flux with DGT versus Zn flux with LASV. Markers as in Fig 1. Error bars as in
816 previous figures. The added straight line is the global regression of the plotted data.

817

818

HIGHLIGHTS

- Different speciation techniques provide complementary information on the system
- AGNES and PIM measure free Zn concentrations, while LSAV and DGT measure fluxes
- A plot of fluxes vs. free concentrations provides dynamic speciation information
- Lability degrees can be computed combining results of speciation techniques